

# 1 **Contrasting drought legacy effects on gross primary productivity in a** 2 **mixed versus pure beech forest**

3  
4 Xin Yu<sup>1</sup>, René Orth<sup>1</sup>, Markus Reichstein<sup>1</sup>, Michael Bahn<sup>2</sup>, Anne Klosterhalfen<sup>3</sup>, Alexander Knohl<sup>3</sup>, Franziska Koebsch<sup>3</sup>, Mirco  
5 Migliavacca<sup>1,4</sup>, Martina Mund<sup>5</sup>, Jacob A. Nelson<sup>1</sup>, Benjamin D. Stocker<sup>6,7</sup>, Sophia Walther<sup>1</sup>, and Ana Bastos<sup>1</sup>

6 <sup>1</sup>Department of Biogeochemical Integration, Max Planck Institute for Biogeochemistry, Jena, D-07745, Germany

7 <sup>2</sup>Department of Ecology, University of Innsbruck, Innsbruck, A-6020, Austria

8 <sup>3</sup>Bioclimatology, University of Göttingen, Göttingen, D-37077, Germany

9 <sup>4</sup>Joint Research Centre, European commission, Ispra (VA), 21027, Italy

10 <sup>5</sup>Forestry Research and Competence Centre Gotha, Gotha, D-99867, Germany

11 <sup>6</sup>Department of Environmental Systems Science, ETH, Zürich, 8092, Switzerland

12 <sup>7</sup>Swiss Federal Institute for Forest, Snow and Landscape Research WSL, Birmensdorf, 8903, Switzerland

13  
14 *Correspondence to:* Xin Yu (xyu@bgc-jena.mpg.de)

15 **Abstract.** Droughts affect terrestrial ecosystems directly and concurrently, and can additionally induce lagged effects in  
16 subsequent seasons and years. Such legacy effects of drought on vegetation growth and state have been widely studied in tree-  
17 ring records and satellite-based vegetation greenness, while legacies on ecosystem carbon fluxes are still poorly quantified and  
18 understood. Here, we focus on two ecosystem monitoring sites in central Germany with similar climate but characterized by  
19 different species and age structures. Using eddy-covariance measurements, we detect legacies on gross primary productivity  
20 (GPP) by calculating the difference between random-forest model estimates of potential GPP and observed GPP. Our results  
21 showed that at both sites, droughts caused significant legacy effects on GPP at seasonal and annual time scales which were  
22 partly explained by reduced leaf development. The GPP reduction due to drought legacy effects is of comparable magnitude  
23 to the concurrent drought effects, but differed between two neighbouring forests with divergent species and age structures. The  
24 methodology proposed here allows quantifying the temporal dynamics of legacy effects at the sub-seasonal scale and  
25 separating legacy effects from model uncertainties. Application of the methodology at a larger range of sites will help quantify  
26 whether the identified lag effects are general and on which factors they may depend.

## 27 **1 Introduction**

28 The frequency, intensity, duration, and spatial extent of drought are expected to increase in the next decades due to  
29 anthropogenic global warming in many regions (IPCC, 2022). A great number of studies, considering both long-term  
30 observations (Schwalm et al., 2010; Zscheischler et al., 2014) and model simulations (Reichstein et al., 2007; Sun et al., 2015)

31 across various spatial scales, have shown that droughts concurrently impact the structure and function of terrestrial ecosystems  
32 (Assal et al., 2016; Frank et al., 2015; Lewis et al., 2011; Ma et al., 2015; Orth et al., 2020), potentially turning ecosystems  
33 from sinks to temporary sources of carbon (Ciais et al., 2005; Reichstein et al., 2013). Therefore, understanding the impact of  
34 droughts on terrestrial ecosystems is a key research question in Earth sciences (Piao et al., 2019).

35 Drought impacts on terrestrial ecosystems are not limited to concurrent effects, but also include legacy effects during the  
36 following seasons and years (Anderegg et al., 2015; Frank et al., 2015; Kannenberg et al., 2020; Müller and Bahn, 2022).  
37 Legacy effects at tree and/or stand scale can be caused by the higher vulnerability to drought due to previous water depletion  
38 of the soil (Krishnan et al., 2006, Galvagno et al., 2013), reduced or delayed leaf development (Migliavacca et al., 2009; Rocha  
39 and Goulден, 2010; Kannenberg et al., 2019), drought-induced hydraulic damage of the xylem (Anderegg et al., 2013),  
40 adjustments in carbon allocation within the trees (Huang et al., 2021), depletion of non-structural carbohydrates (Peltier et al.,  
41 2021) due to reduced carbon availability and adjustments in carbon allocation (Hartman and Trumbore, 2016), tree mortality  
42 (Allen et al., 2015), as well as reduced resistance to disturbances (e.g. insects outbreaks) due to depleted non-structural  
43 carbohydrates (Erbilgin et al., 2021). However, at the ecosystem level the impact of species and age structures on legacy effects  
44 are still less understood (Haberstroh and Werner, 2022, Wang et al., 2022).

45 Tree-ring records cover periods of decades to centuries and can cover multiple drought events, being therefore widely used to  
46 analyze inter-annual legacy effects of drought on tree growth (Anderegg et al., 2015; Huang et al., 2018; Kannenberg et al.,  
47 2019). Beyond the level of individual trees, satellite-based observations and model outputs, as expressed through vegetation  
48 greenness (Wolf et al., 2016; Wu et al., 2018), canopy backscatter (Saatchi et al., 2013), aboveground carbon stocks (Wigneron  
49 et al., 2020), and gross primary productivity (Schwalm et al., 2017, Bastos et al., 2020) have also been used to study seasonal  
50 and inter-annual legacy effects of drought. However, studies focusing on carbon fluxes, especially based on eddy-covariance  
51 measurements, are still rare (Kannenberg et al., 2020). Eddy-covariance data with hydrometeorological variables measured in  
52 parallel have the potential to quantify the timing and magnitude of legacy effects at the sub-seasonal and annual scales, and  
53 might provide insights into the mechanisms of legacy effects that might not be fully reflected in vegetation indices and tree  
54 rings.

55 Assessments of drought impacts on the ecosystem carbon fluxes usually focus on direct and concurrent effects (Ciais et al.,  
56 2005; Reichstein et al., 2007) without considering legacy effects. This is probably due to the challenge to attribute signals in  
57 the observations to a previous drought and hence identify them as legacy effects on ecosystem carbon fluxes (Kannenberg et  
58 al., 2020), and the inability of models to reproduce these legacy effects (Bastos et al., 2021). A number of studies consider  
59 ecosystems to have ‘recovered’ when the target variable such as gross primary productivity (GPP) and tree-ring width returns  
60 to the baseline, which is usually based on pre-drought values of the target variable (Bose et al., 2020; González de Andrés et  
61 al., 2021; Zhang et al., 2021). However, this might complicate the detection of legacies since GPP recovery dynamics is  
62 affected by hydrometeorological conditions in legacy years, which can either stimulate or slow-down recovery. Here, by  
63 estimating potential GPP given hydrometeorological conditions in legacy years, we consider that ‘recovery’ happens when the  
64 actual GPP reaches the potential GPP under the given hydrometeorological conditions, rather than the absolute flux.

65 Therefore, we aimed to develop a novel approach to quantify drought legacy effects on GPP at the sub-seasonal and annual  
66 scales. To do this, we followed a residual approach (Beringer et al., 2007) to identify legacy effects as the residuals between  
67 actual and potential GPP which is estimated by a machine-learning algorithm (specifically Random Forest regression).  
68 Furthermore, it is crucial to understand if the residuals are caused by model uncertainties or can be interpreted as legacy effects.  
69 By overlooking model uncertainties, one could misinterpret small residuals as ‘legacy effects’. Here we quantified model  
70 uncertainties to provide more robust estimates of drought legacies and avoid misinterpretation of results. To test our approach,  
71 we used eddy-covariance measurements at two neighbouring sites that experienced similar climate but are characterized by  
72 different species and age structures in central Germany. We asked 1) can we detect drought legacy effects on GPP? 2) is the  
73 GPP reduction due to drought legacy effects significant compared to the magnitude of drought concurrent effects? 3) how do  
74 drought legacy effects on GPP differ at two neighbouring forests with different species and age structures?

## 75 **2 Data**

### 76 **2.1 Study sites**

77 The two neighboring temperate forest sites studied here, Hainich (DE-Hai, 51°04'46"N, 10°27'07"E) and Leinefelde (DE-Lnf,  
78 51°19'42"N, 10°22'04"E), are located in central Germany, approximately 30 km from each other. These two sites share similar  
79 climate conditions, with long-term annual mean of 8 °C for 2-m air temperature and 750 mm of total annual precipitation  
80 (Tamrakar et al., 2018). Both sites were affected by the two extreme central European droughts in 2003 and 2018 which  
81 reduced gross primary productivity (Fu et al., 2020; Herbst et al., 2015).

82 The forest at Hainich is an old-growth, uneven aged (1-250 years) mixed forest, dominated by beech (*Fagus sylvatica*,  
83 representing approximately 64% of the tree carbon stocks). Ash (*Fraxinus excelsior*, 28%) and sycamore (*Acer*  
84 *pseudoplatanus*, 7%) are co-dominant tree species, and additionally there are few trees of European hornbeam (*Carpinus*  
85 *betulus*), Norway maple (*Acer platanoides*), and other deciduous species (Knohl et al., 2003). The forest at Leinefelde can be  
86 characterized as a managed even-aged (ca. 130 years) pure beech forest (Anthoni et al., 2004).

### 87 **2.2 Eddy-covariance and meteorological measurements**

88 Identical eddy-covariance instrumental setups and data acquisition techniques were carried out at the two sites. The  
89 methodology of data collection and quality control followed those of Aubinet et al. (2000). The standard processing methods  
90 (Pastorello et al., 2020) adopted by the Integrated Carbon Observation System (ICOS) were used to carry out the gap-filling  
91 and the partitioning (Warm Winter 2020 Team and ICOS Ecosystem Thematic Centre 2022). The GPP estimated from the  
92 nighttime partitioning algorithm (Reichstein et al., 2005) was used for the analysis (GPP\_NT\_VUT\_REF). A detailed  
93 description of meteorological data and instrumentation can be found in previous studies (Anthoni et al., 2004; Knohl et al.,  
94 2003). We used daily meteorological data alongside carbon and water fluxes, namely GPP, latent heat flux after the energy  
95 balance correction (LE\_CORR), which was converted to evapotranspiration (ET) using the heat of vaporization, incoming

96 shortwave radiation (SW\_IN), air temperature (TA), vapor pressure deficit (VPD), soil water content at the first layer (SWC\_1,  
97 8cm), the second layer (SWC\_2, 16cm), the third layer (SWC\_3, 32cm), and potential incoming shortwave radiation  
98 (SW\_IN\_POT) for the years 2000-2020 at DE-Hai and 2002-2012, with a gap in 2007-2009, at DE-Lnf.  
99 Additionally, we used daily enhanced vegetation index (EVI) data from the FluxnetEO v1.0 dataset (Walther et al., 2021) for  
100 the same years as the eddy-covariance data. EVI was derived from the MCD43A4 product of MODIS with a 500m spatial  
101 resolution and we used an average over 2x2 pixels surrounding the tower. We further estimated daily transpiration based on  
102 the Transpiration Estimation Algorithm (Nelson et al., 2018).

### 103 **2.3 Radial increment and net primary productivity of fruits and leaves**

104 Annual radial increment (RI) was calculated from permanent band dendrometers which measures change in stem girth (or  
105 circumference) over bark. The effect due to the inclusion of shrinkage and swelling of the bark is a negligible uncertainty for  
106 four reasons: 1) we used only the annual increment, 2) the dominant species is beech that has only a thin bark, 3) we recorded  
107 the final stem diameter of each year in winter, when the water status of the xylem and the bark is relatively constant, and when  
108 stem wood or the bark are not affected by frost or late/early growth or water uptake, and 4) in this study we were interested  
109 only in the interannual variability of stem growth, which is less affected by shrinkage and swelling at the described temporal  
110 scale than absolute growth rates. The dendrometer trees represented the main species and their respective size classes of the  
111 main footprint at DE-Hai for the years 2003 to 2020. Because of technical constraints, damages and a natural dieback of single  
112 trees, the number of measurement trees per year varied between 54 and 95. Net primary productivity (NPP) of fruits for the  
113 years 2003 to 2020, and NPP of leaves for the years 2003 to 2016 resulted from litter samplings (25-29 traps) within the main  
114 footprint area of the flux tower. The high fluctuation of annual fruit NPP is caused by the periodically high fruit production  
115 (masting) of beech (*Fagus sylvatica*). In most years the proportion of beech fruits (nuts and shells) amounted to almost 92%  
116 of total fruit mass. At DE-Lnf these data are not available. A detailed description of measurement and processing methods can  
117 be found in a previous study (Mund et al., 2020).

## 118 **3 Methodology**

### 119 **3.1 Data processing**

120 As the first step, we filtered and processed the eddy covariance and meteorological data in the following way:

- 121 1) To ensure reliable data for our analysis we used gap-filled daily data for days for which more than 70% of measured and  
122 good quality gap-fill data (Reichstein et al., 2005) were available.
- 123 2) We only used data during the growing season which was defined as the period when GPP was greater than 10% of maximum  
124 of GPP as inferred from a smoothed (centered 7-days moving averages) daily average GPP across all years.

125 3) We calculated anomalies of all variables by subtracting the mean seasonal cycle and any significant long-term linear trend,  
126 detected by the Mann-Kendall test (Kendall, 1948), as these can obscure drought-related signals. We took the mean of each  
127 day across all considered years and then used centered 7-days moving averages to calculate the mean seasonal cycle.

128 4) Furthermore, a 7-days moving average smoothing was applied to the anomaly time series to filter out noise at daily time  
129 scales. We expect this to increase the accuracy of our model while preserving drought legacy patterns which rather/better  
130 emerge at longer time scales.

131 As for RI data, we removed for each individual tree any significant long-term linear trend detected using the Mann-Kendall  
132 test (Kendall, 1948).

133

### 134 **3.2 Water availability index estimation**

135 Soil moisture at the two study sites was measured only at the upper 30 cm and thus does not account for water availability in  
136 deeper layers (see Section 5.4). Therefore, we used a bucket model approach based on observed evapotranspiration and  
137 precipitation to estimate a vegetation water availability index, WAI (Tramontana et al., 2016), calculated as:

$$WAI_0 = WAI_{\text{warm-up}} \quad (1)$$

$$WAI_t = \min(WAI_{\text{max}}, WAI_{t-1} + P_t - ET_t) \quad (2)$$

138 Where  $WAI_0$  was the initial value of the water availability index (WAI),  $WAI_{\text{warm-up}}$  was the end value of WAI from the warm-  
139 up of the bucket model (Eq. 1). To warm up the bucket model, we ran it 5 times through the first year before starting the actual  
140 computation across all considered years.  $WAI_{t-1}$  (mm) and  $WAI_t$  (mm) were WAI at time step  $t-1$  and  $t$ , respectively,  $P_t$  (mm),  
141 and  $ET_t$  (mm) were, precipitation, and evapotranspiration at time step  $t$  (Eq. 2). We set the bucket size (i.e.  $WAI_{\text{max}}$ ) as the  
142 maximum cumulative water deficit (CWD) at each site. The estimated bucket sizes were 205 mm and 191mm at DE-Hai and  
143 DE-Lnf, respectively.

144 Additionally, we calculated the CWD, which was estimated from cumulative differences between observed evapotranspiration  
145 and precipitation over periods where cumulative net water loss from the soil ( $\Sigma (ET-P)$ ) is positive.

### 146 **3.3 Drought and legacy years selection**

147 Since legacy effects should result from significant impacts of droughts on ecosystems, we adopted a combined driver and  
148 impact-based approach to define droughts. Drought years were defined as those years when both low water availability and a  
149 concurrent biospheric response were found, and were evaluated as follows:

150 1) First, we selected the minimum of negative GPP anomalies relative to the mean seasonal cycle during the growing season  
151 (minimum  $GPP_{\text{anom}}$ ) as a proxy to reflect the severity of drought impact on GPP in each year.

152 2) Then, we calculated the mean WAI anomalies relative to the mean seasonal cycle for days when minimum  $GPP_{\text{anom}}$  occurred  
153 and the previous 14 days (mean  $WAI_{\text{anom}_{15}}$ ) to reflect the water availability during the development of the GPP anomaly. To

154 identify drought-related GPP reductions, we considered only years where negative GPP anomalies were associated with dry  
155 conditions.

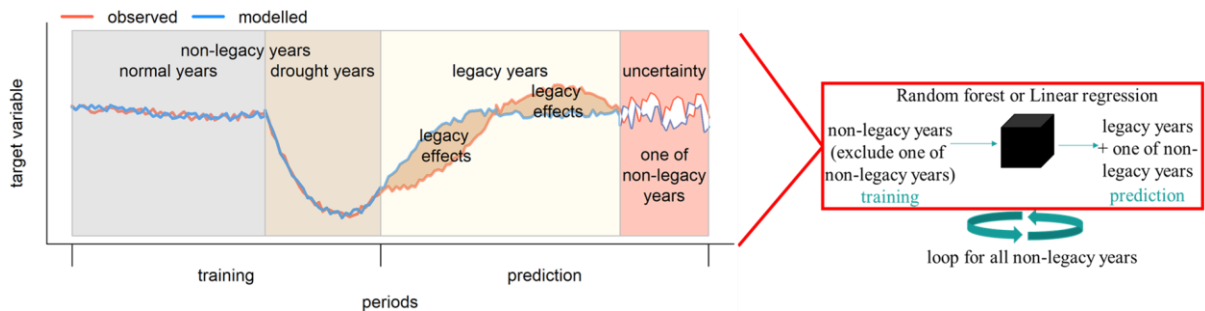
156 3) Finally, we selected the years with both the lowest minimum  $GPP_{anom}$  and mean  $WAI_{anom_{15}}$  (Fig. S1). These were 2003 and  
157 2018 at DE-Hai and 2003 at DE-Lnf (2018 data not available here).

158 In our data, we define non-legacy years as normal and drought years, while legacy years correspond to the two calendar years  
159 following a drought year. Including too few legacy years could lead to an underestimation of legacy effects, and too many  
160 legacy years would result in the lack of training data (see Section 3.4). As a trade-off, we selected a legacy period of two years  
161 and this choice was justified by the fact that GPP anomalies residuals returned to the range of model uncertainties (i.e. 25<sup>th</sup>-  
162 75<sup>th</sup> percentiles of model residuals), which is considered as the point when GPP recovers. This happened in 2005 (see Section  
163 4.3) following the 2003 drought at both sites. For the 2018 drought at DE-Hai, data was only available up to 2020.

### 164

### 165 3.4 Quantification of legacy effects on GPP and transpiration

166 Here, we followed a residual approach (Beringer et al., 2007) to detect drought legacy effects on GPP. To do this, we fitted a  
167 random forest regression model (RF, Breiman 2001) for daily GPP anomalies using the anomalies of hydro-meteorological  
168 variables in non-legacy years as predictors. We chose RF because it has the ability to effectively learn 1) the relationship  
169 between independent and dependent variables regardless of linear or non-linear relationships; 2) the interactions between  
170 independent variables (Ryo and Rillig, 2017). The model was then used to predict GPP anomalies in the legacy years, thereby  
171 reflecting the potential GPP anomalies given the climate conditions in that year. Specifically, the approach included the  
172 following steps (Fig. 1):



173  
174 **Figure 1. Conceptual diagram of quantification of legacy effects.** A random forest (RF) model (or linear regression, represented by the  
175 black cube on the right) was used to determine the relationship between the target variable ( $GPP_{anom}$  or RI) and hydro-meteorological  
176 conditions using a training dataset excluding data in legacy years and one of non-legacy years for each loop. The legacy effects could be  
177 quantified as the residuals between observed (red line) and modelled (blue line) target variable (i.e.  $GPP_{anom}$ , RI, ...). And  
178 the residuals between observed and modelled target variable (i.e.  $GPP_{anom}$ , RI, ...) in all non-legacy years from all loops indicated RF model  
179 uncertainties using a leave-one-out approach (see below).

180 First, all daily data in non-legacy years were used as input for the RF model to determine the relationships between anomalies  
181 of GPP ( $GPP_{anom}$ ) and anomalies of hydro-meteorological variables ( $SW\_IN_{anom}$ ,  $TA_{anom}$ ,  $VPD_{anom}$ , and  $WAI_{anom}$ ) along with  
182 absolute values of  $SW\_IN\_POT$  to capture seasonal variations in the response of ecosystems to hydro-meteorological

183 conditions. These relationships represented long-term controls of climate on GPP, including drought events and near-average  
184 or wet conditions. The Out of bag (OOB) scores indicating the prediction ability of RF models were  $\sim 0.7$  and  $\sim 0.8$  (where zero  
185 indicates no skill and 1 denotes perfect performance) at DE-Hai and DE-Lnf, respectively (Fig. S2).  $WAI_{anom}$  is the most  
186 important explanatory factor at both sites, followed by  $SW\_IN_{anom}$  at DE-Hai and the phenological stage (given by  
187  $SW\_IN\_POT$ ) at DE-Lnf (Fig. S3). The ‘randomForest’ package in R 4.0.3 was used, and the number of trees, the number of  
188 variables randomly sampled as candidates at each split, and the node size of RF were set to 400, 5, and 5, respectively. Tuning  
189 those hyperparameters did not significantly change our results.

190 Based on these relationships and the meteorological anomalies in legacy years, we used the trained RF model to predict the  
191 potential  $GPP_{anom}$  in the absence of legacy effects and calculated the model's residuals ( $GPP_{anom}$  residuals, i.e. observed minus  
192 predicted values), which should reflect legacies from the past drought: negative residuals corresponded to more negative or  
193 less positive  $GPP_{anom}$  than would be expected given the meteorological conditions in that year, indicating negative legacies  
194 of drought, while positive residuals corresponded to less negative or more positive  $GPP_{anom}$ , indicating beneficial legacies of  
195 drought. In order to reduce the noise at the daily scale, daily results were aggregated to the weekly scale.

196 To account for model uncertainties and evaluate the significance of legacy effects, we used a leave-one-out approach to  
197 quantify model uncertainties. In the training phase, one of the non-legacy years was excluded from the training dataset and the  
198 trained RF model was then used to predict the  $GPP_{anom}$  in that year. This was done for all non-legacy years, and the  $GPP_{anom}$   
199 residuals in non-legacy years for each leave-one-out iteration were then considered as model uncertainties. In order to reduce  
200 the noise at the daily scale, all the daily results were aggregated to the weekly scale.

201 In order to infer possible legacy effects due to plant hydraulic damage, the same method was used to quantify legacy effects  
202 on transpiration ( $Tr$ ) estimated by TEA (Transpiration estimation algorithm) approach (Nelson et al., 2018). The TEA approach  
203 first isolates the periods when evapotranspiration is most likely dominated by transpiration. Then, a quantile random forest  
204 model (Breiman, 2001; Meinshausen and Ridgeway 2006) is trained during the separated periods and transpiration can be  
205 estimated at every time step. More detail can be found in Nelson et al., 2018. We use  $Tr$ , rather than evapotranspiration ( $ET$ )  
206 because decreases in  $Tr$  due to hydraulic damage could be offset by increased soil evaporation, making the aggregated  $ET$   
207 signal difficult to interpret.

### 208 **3.5 Quantification of legacy effects on tree growth**

209 To detect legacy effects on tree growth, we used a multivariate-linear regression instead of RF to develop the relationship  
210 between tree growth (detrended radial increment,  $RI$ ) due to the fewer data points available. We used the following explanatory  
211 variables: detrended growing-season mean  $WAI$ , detrended growing-season mean  $VPD$ , detrended growing-season mean  
212  $SW\_IN$ , and detrended growing-season mean  $TA$  for each species. We detrended the time series of all variables by removing  
213 any significant long-term linear trend detected using the Mann-Kendall test (Kendall, 1948). Annual net primary productivity  
214 of fruits (fruits-NPP) particularly was added as an additional predictor to only the model for beech since the high fluctuation  
215 of annual fruit NPP could be caused by the periodically high fruit production (masting) of beech. We considered fruits-NPP

216 as a predictor to account for the trade-off between tree growth and reproduction in mast years, which could also cause the  
217 change in tree growth in addition to legacy effects from previous droughts (Hackett-Pain et al., 2015).  
218 The strategy to quantify legacy effects and model uncertainties was the same as in the case of GPP. We trained the model in  
219 non-legacy years except for each one of them iteratively and predicted potential RI in legacy years and the year additionally  
220 excluded. The residuals between observed and potential RI in non-legacy years and legacy years were then considered as  
221 model uncertainties and legacy effects, respectively.

### 222 **3.6 Separation of legacy effects on GPP due to structural and physiological effects**

223 Drought legacy effects on GPP might result from changes in canopy structure (structural effects) and photosynthesis capacity  
224 (physiological effects) (Kannenbergh et al., 2019). Combining GPP and satellite-based EVI allows separating these structural  
225 and physiological effects. To do this separation, we used two model settings: 1) RF, which was the original setting described  
226 in section 3.4, included both structural and physiological effects; 2) RF<sub>EVI</sub>, which added EVI anomalies as an additional  
227 predictor to the original model, only included physiological effects because structural effects were already included in the  
228 predictor EVI anomalies and GPP<sub>anom</sub> residuals from this model were expected to be caused by physiological effects. Therefore,  
229 physiological legacy effects on GPP were quantified as GPP<sub>anom</sub> residuals from RF<sub>EVI</sub> while structural legacies were quantified  
230 as the difference between GPP<sub>anom</sub> residuals from RF and RF<sub>EVI</sub> (i.e. RF-RF<sub>EVI</sub>). The same method was used to separate  
231 structural and physiological effects of legacy effects on Tr.

### 232 **3.7 Quantifying concurrent and lagged reduction in GPP from drought**

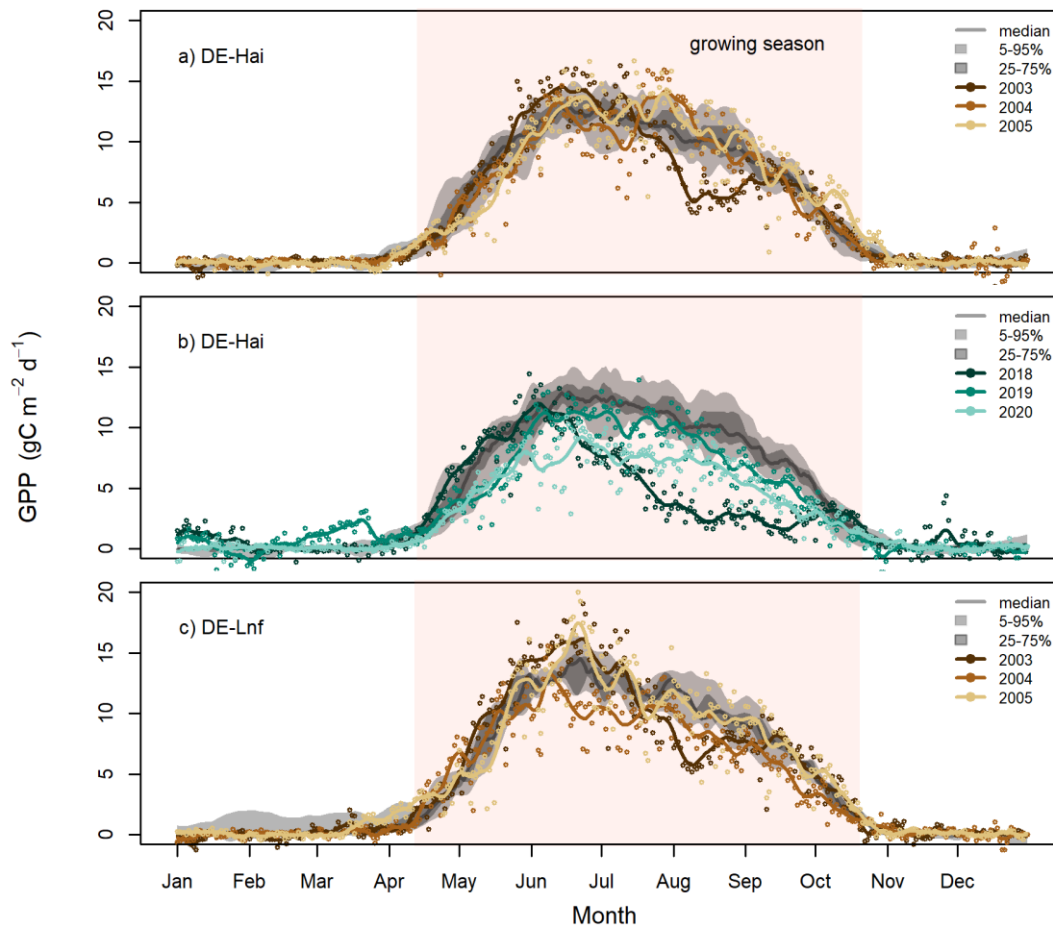
233 Additionally, we compared the estimated legacy effects on GPP to the concurrent drought-induced GPP anomalies. To compute  
234 the concurrent reduction in GPP, we summed up all GPP anomalies over each identified drought period. Here, drought periods  
235 were defined as the periods where WAI<sub>anom</sub> was lower than -1 of standard deviation (WAI<sub>SD</sub>). WAI<sub>SD</sub> was calculated for each  
236 day of year by using a centered 7-day moving window instead of a single value over the whole time series because WAI<sub>SD</sub>  
237 showed a seasonality. This definition only relied on the water availability without considering biospheric responses because  
238 WAI directly indicated the water supply for vegetation while GPP could include other factors in addition to drought in short  
239 periods. We quantified the lagged reduction in GPP at the annual scale as the difference between GPP<sub>anom</sub> residuals in legacy  
240 years and the median of the model uncertainties. To compare the reduction in GPP across sites, both concurrent and lagged  
241 values were normalized relative to averaged total GPP over the growing season.

## 242 **4. Results**

### 243 **4.1 GPP time series in drought and legacy years**

244



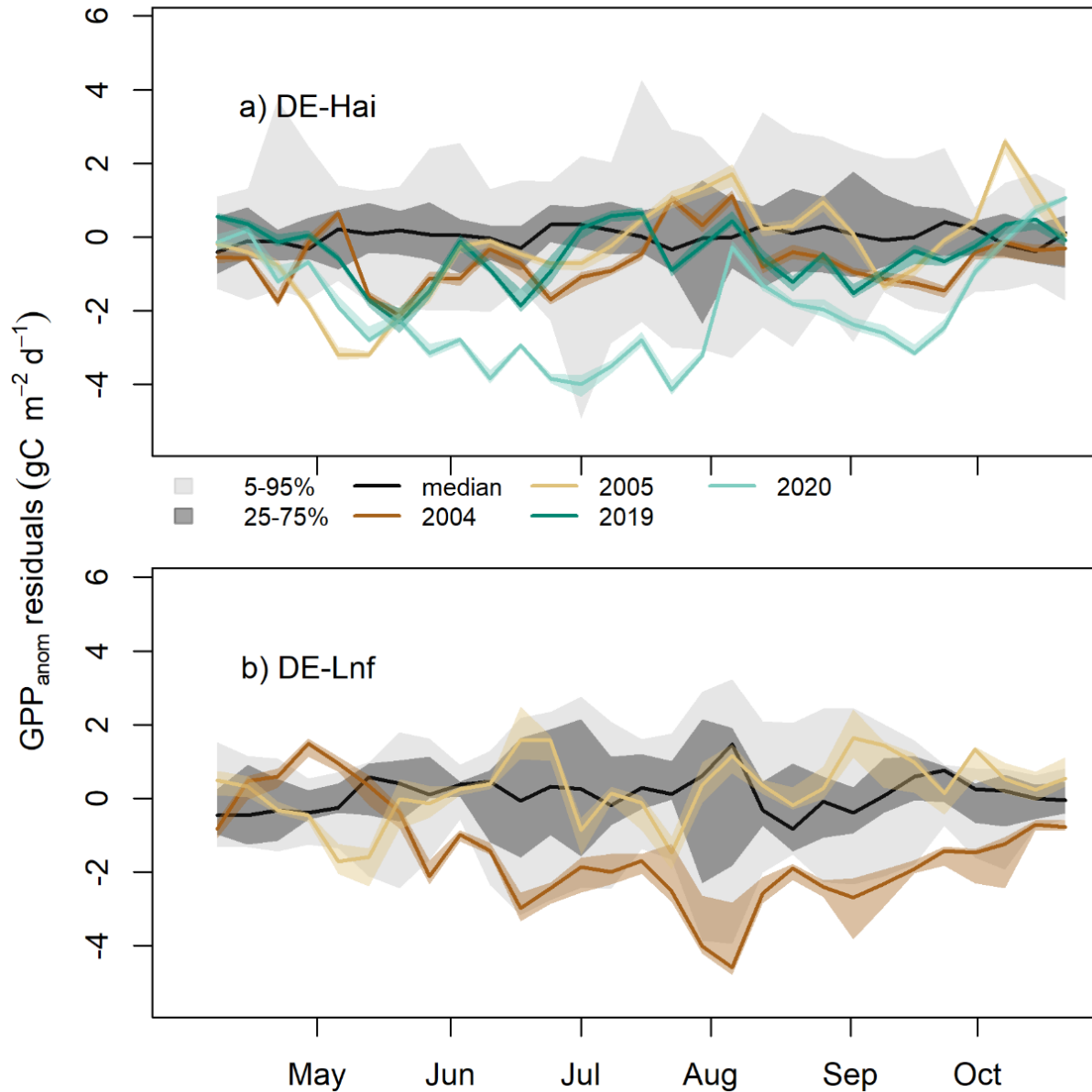


245

246 **Figure 2. Daily GPP in the selected drought and legacy years at a) DE-Hai 2003, b) DE-Hai 2018 and c) DE-Lnf 2003 showing the**  
 247 **droughts and following legacy years, respectively.** Colored points and lines showed original and smoothed (7-days average) GPP,  
 248 respectively, in drought and legacy years. The grey lines and shaded areas showed the median, 25<sup>th</sup>-75<sup>th</sup> (dark grey), and 5<sup>th</sup>-95<sup>th</sup> (light grey)  
 249 percentiles of GPP, respectively, over non-drought and non-legacy years. The shaded coral areas indicate the average growing seasons of  
 250 DE-Hai and DE-Lnf.

251 In Fig. 2, we show the measured absolute GPP time series in the selected drought (2003 and 2018) and legacy years (2004,  
 252 2005, 2019, and 2020) together with the long-term median, 25<sup>th</sup>-75<sup>th</sup>, and 5<sup>th</sup>-95<sup>th</sup> percentiles GPP at DE-Hai and DE-Lnf. In  
 253 the drought year 2003, GPP was significantly lower than the baseline, defined as the 25<sup>th</sup> percentile GPP, during July-  
 254 September at DE-Hai and July-August at DE-Lnf, respectively. In the post-drought years 2004 and 2005, there was no  
 255 systematic decrease in GPP at DE-Hai, while GPP at DE-Lnf was slightly lower than the baseline during June-August of 2004.  
 256 During the 2018 drought, GPP significantly differed from the baseline during June-September at DE-Hai. After the 2018  
 257 drought, we could not find any systematic decrease in GPP in 2019, while GPP was consistently lower than the baseline from  
 258 mid-May to September of 2020 at DE-Hai.

259



261

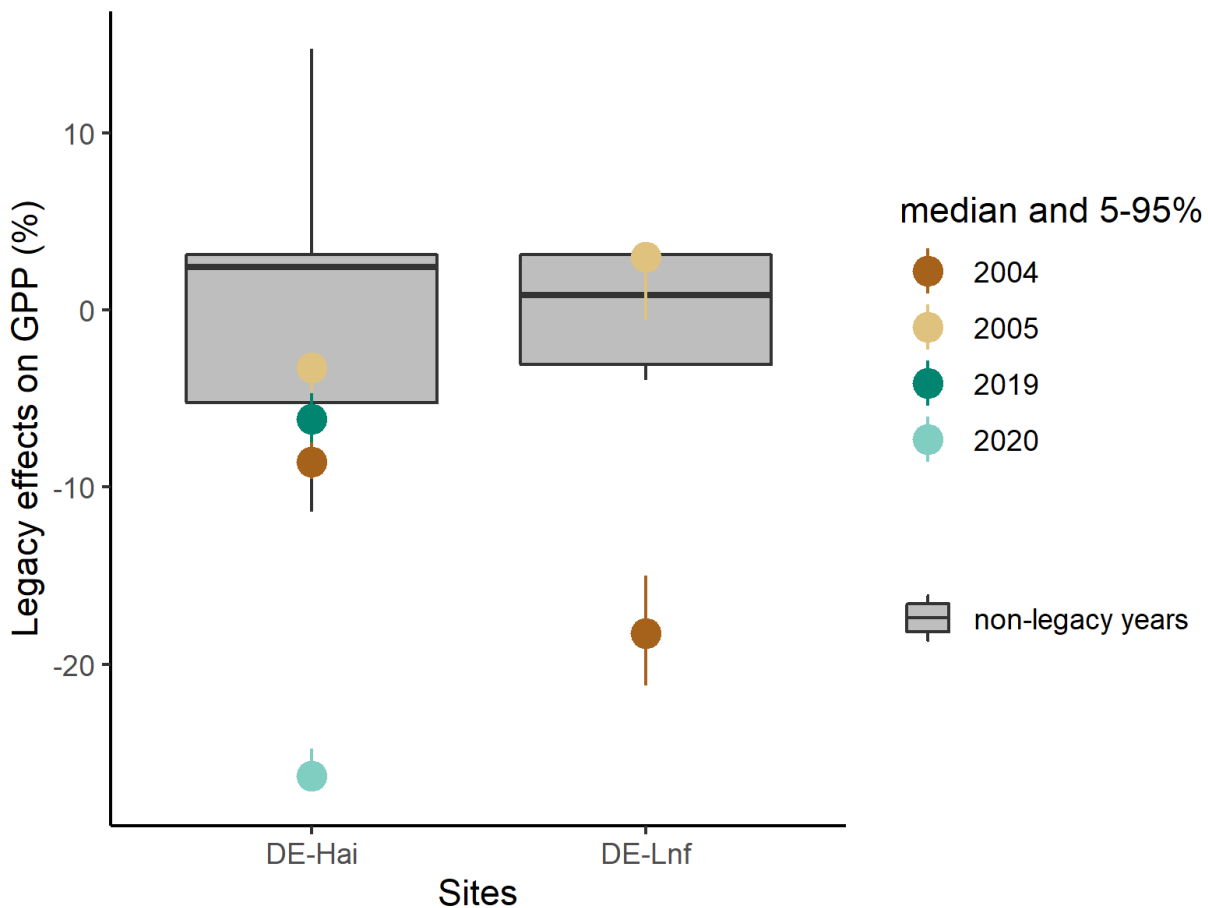
262 **Figure 3. Residuals of GPP anomalies at the seasonal scale in legacy years at a) DE-Hai and b) DE-Lnf.** Residuals of GPP anomalies  
 263 were characterized by observed minus predicted GPP anomalies (GPP<sub>anom</sub> residuals). The color lines and bands show the median and 5<sup>th</sup>-  
 264 95<sup>th</sup> percentile GPP<sub>anom</sub> residuals of ensemble model runs (see Section 3.4), respectively. Negative residuals corresponded to more negative  
 265 or less positive GPP<sub>anom</sub> than would be expected given the climate in that year, indicating negative legacies of drought, while positive  
 266 residuals corresponded to less negative or more positive GPP<sub>anom</sub>, indicating beneficial legacies of drought. The model uncertainties (dark  
 267 and light grey shaded area, respectively) are characterized by the 25<sup>th</sup>-75<sup>th</sup> and 5<sup>th</sup>-95<sup>th</sup> quantile ranges of GPP<sub>anom</sub> residuals in non-legacy  
 268 years. The black line represents the median of GPP<sub>anom</sub> residuals in non-legacy years. The ticks denote the start of each month.

269 At the seasonal scale, residuals of GPP anomalies ( $GPP_{anom}$  residuals) showed significant departures from model uncertainties  
 270 at both sites (Fig. 3). After the 2003 drought at DE-Hai, we found negative residuals below the 25<sup>th</sup> percentile of model  
 271 residuals in non-legacy years (model uncertainties) during the early and late growing season of 2004 (April-July, September)  
 272 and May-June of 2005, and below the 5<sup>th</sup> percentile for short periods, in April and May of 2004 and May of 2005. After June  
 273 2005, residuals were mostly within 5-95% of the model residuals. After the 2018 drought at DE-Hai, we found negative  
 274 residuals (below 25<sup>th</sup> percentile of model residuals) during May, June, August, and September of 2019. In 2020, residuals  
 275 showed a persistent decrease from May to July, and generally stayed well below the 5<sup>th</sup> and 25<sup>th</sup> percentile of model residuals  
 276 from mid-May until July and September, respectively.

277 After the 2003 drought at DE-Lnf, we found persistent negative residuals were below the 25<sup>th</sup> percentile of model residuals  
 278 over almost the complete growing season (from May to October) in 2004 and below the 5<sup>th</sup> percentile of model residuals for  
 279 periods in June-September. In 2005, residuals remained mostly within 25<sup>th</sup>-75<sup>th</sup> percentiles of model residuals.

280

281 **4.3 Drought legacy effects on GPP: annual patterns**

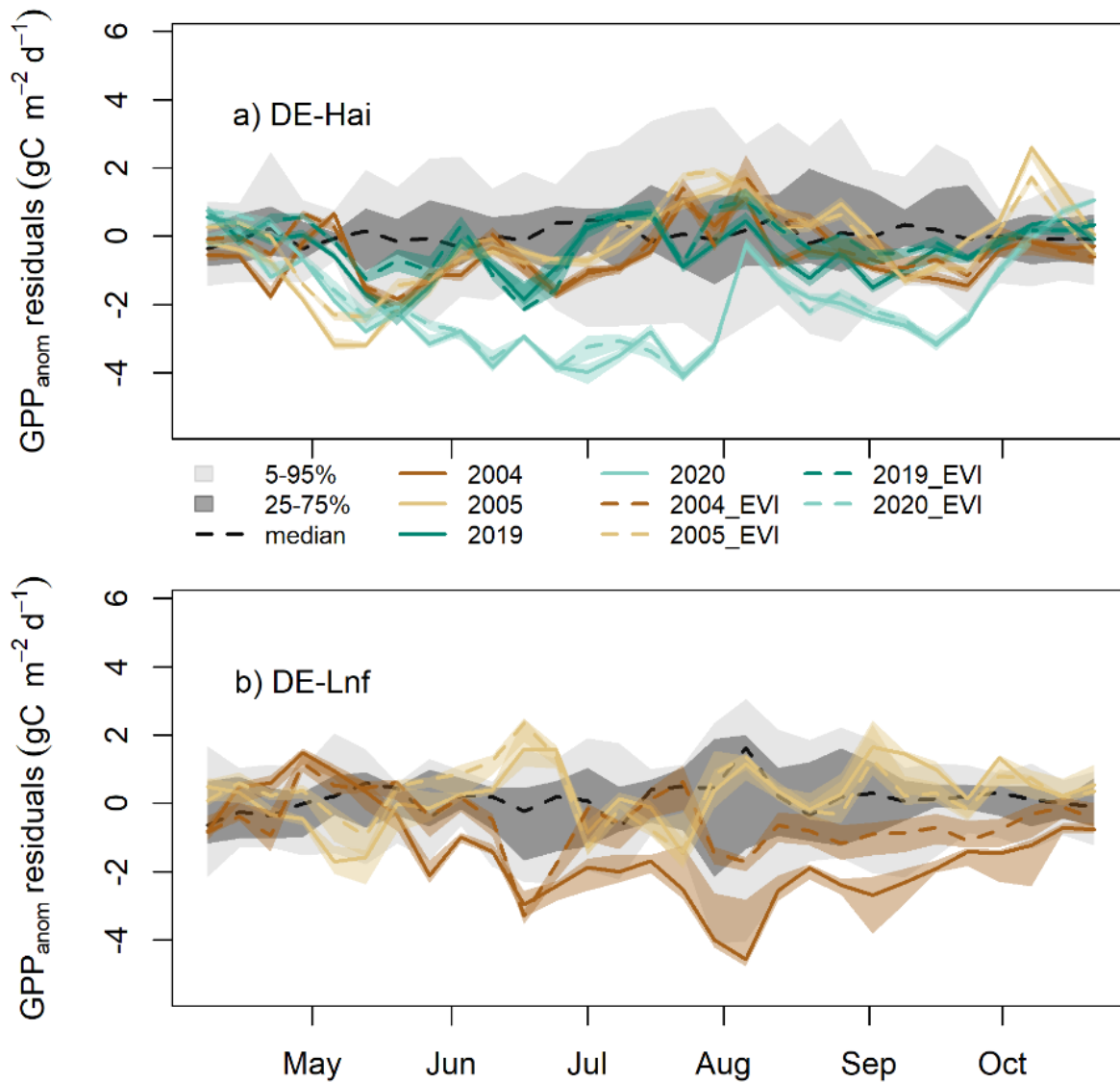


282

283 **Figure 4. Integrated residuals of GPP anomalies at the annual scale in legacy years at DE-Hai and DE-Lnf.** The color points and line  
284 ranges show the median and 5-95% percentile integrated  $GPP_{anom}$  residuals of ensemble model runs (see Section 3.4), respectively. The  
285 model uncertainties (the boxplot) are characterized as the 25<sup>th</sup>-75<sup>th</sup> quantile range of integrated  $GPP_{anom}$  residuals in non-legacy years.

286 There were systematic departures of integrated residuals of GPP anomalies in legacy years from model uncertainties at the  
287 annual scale (Fig. 4) although the seasonal patterns varied (Fig. 3). After the 2003 drought at DE-Hai, integrated residuals in  
288 2004 were significantly below the 25<sup>th</sup> percentile of model residuals, while integrated residuals were within the 25<sup>th</sup>-75<sup>th</sup>  
289 percentiles of model residuals in 2005. After the 2018 drought, integrated residuals in 2019 were near the 25<sup>th</sup> percentiles of  
290 model residuals, while in 2020 integrated residuals were far below the 25<sup>th</sup> percentile of model residuals.

291 At DE-Lnf, after the 2003 drought, integrated residuals in 2004 were below the 25<sup>th</sup> percentile of residuals in non-legacy  
292 years, while integrated residuals almost remained within 25<sup>th</sup>-75<sup>th</sup> percentiles of model residuals in 2005.



294

295 **Figure 5. Residuals of GPP anomalies from RF and RF<sub>EVI</sub> (see Section 3.6) in legacy years at a) DE-Hai and b) DE-Lnf.** Residuals of  
 296 GPP anomalies are characterized by observed minus predicted GPP anomalies (GPP<sub>anom</sub> residuals). The color lines and bands show the  
 297 median and 5<sup>th</sup>-95<sup>th</sup> percentile GPP<sub>anom</sub> residuals of ensemble model runs (see Section 3.4), respectively. The solid and dashed lines show  
 298 the residuals based on RF and RF<sub>EVI</sub>, respectively. The model uncertainties from RF<sub>EVI</sub> (dark and light grey shaded area, respectively) are  
 299 characterized by the 25<sup>th</sup>-75<sup>th</sup> and 5<sup>th</sup>-95<sup>th</sup> quantile ranges of GPP<sub>anom</sub> residuals in non-legacy years. The black dashed line was the median  
 300 of GPP<sub>anom</sub> residuals from RF<sub>EVI</sub> in non-legacy years. The ticks denoted the start of each month. Figure S4 shows the results for April-June  
 301 and August-October at DE-Hai in more detail.

302

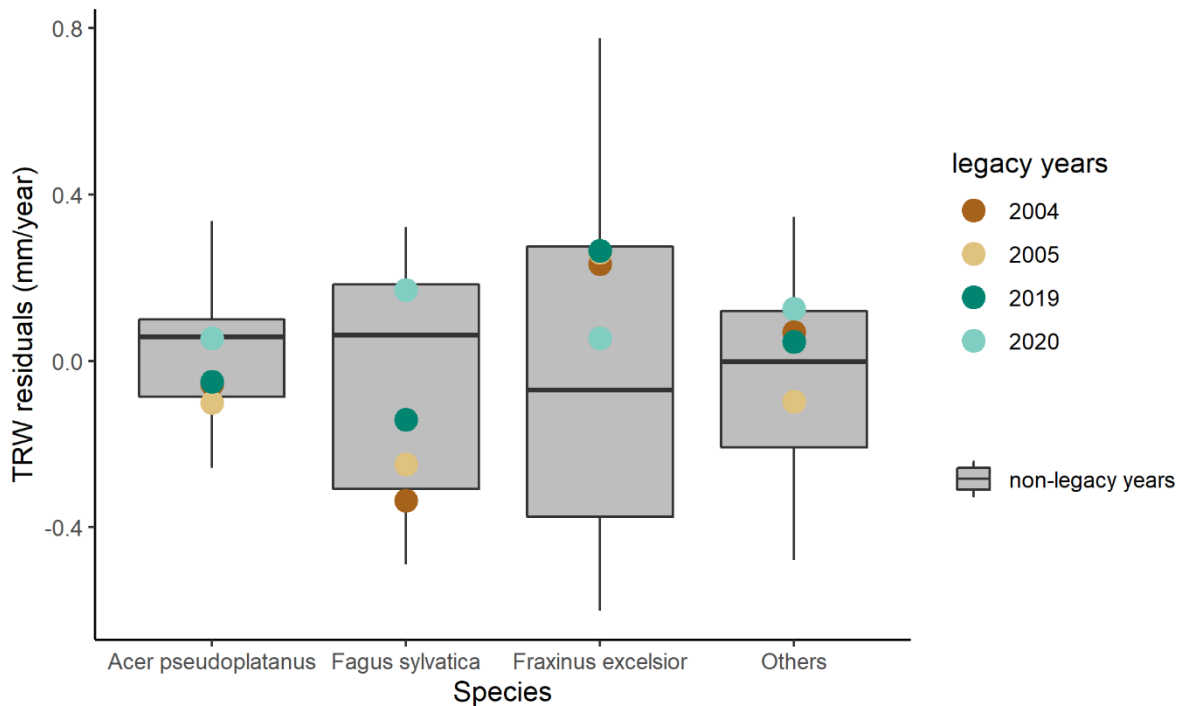
At the seasonal scale, residuals of GPP anomalies from RF<sub>EVI</sub> (Res<sub>EVI</sub>) showed significant departures from GPP<sub>anom</sub> residuals  
 303 from RF (Res) over some periods at both sites (Fig. 5). At DE-Hai, we found Res<sub>EVI</sub> was above Res in the early growing season

304 (April-May) of 2004, 2005, 2019, and 2020, and also in the late growing season of 2004 (August-October) and 2019 (August-  
 305 September). After the 2003 drought, we found negative  $Re_{SEVI}$  below the 25th percentile of model residuals from  $RF_{EVI}$  in  
 306 non-legacy years (model uncertainties) during the early and late growing season of 2004 (May-July, September) and May of  
 307 2005, and below the 5<sup>th</sup> percentile for short periods, in May of 2005. After the 2018 drought, we found negative  $Re_{SEVI}$  (below  
 308 25<sup>th</sup> percentile of model residuals) during June of 2019. In 2020,  $Re_{SEVI}$  showed a persistent decrease from May to July, and  
 309 generally stayed well below the 5<sup>th</sup> and 25<sup>th</sup> percentile of model residuals from mid-May until July and September, respectively.  
 310 At DE-Lnf,  $Re_{SEVI}$  was below Res from April to mid-May and significantly above Res almost over the growing season of 2004  
 311 (from mid-May to September). We found negative  $Re_{SEVI}$  below the 25th percentile of model residuals from  $RF_{EVI}$  in non-  
 312 legacy years (model uncertainties) during June, August, and September of 2004, and below the 5<sup>th</sup> percentile for short periods,  
 313 in June and September of 2004.

314

#### 315 4.5 Drought legacy effects on radial increment

316

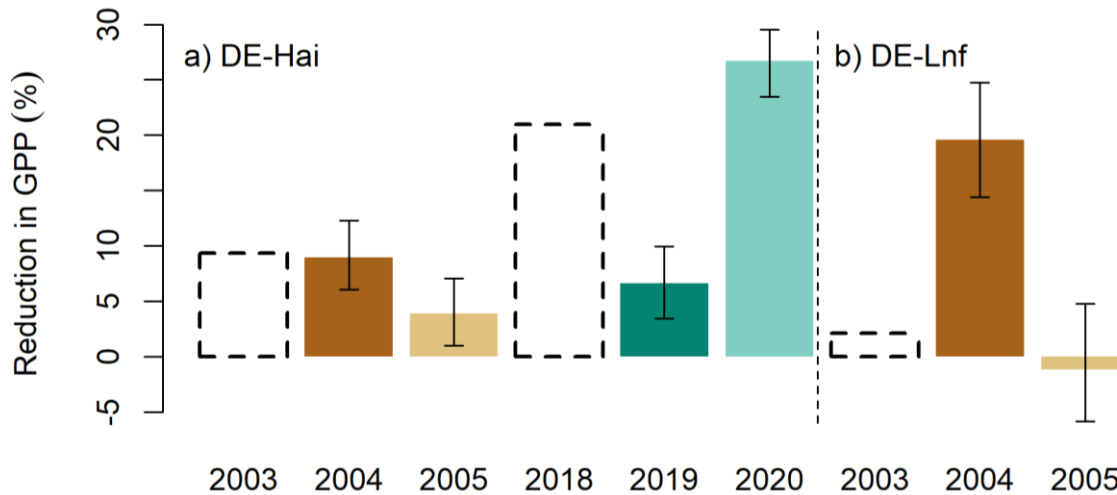


317

318 **Figure 6. Residuals of RI in legacy years at DE-Hai across species.** Residuals of RI are characterized as observed minus predicted RI  
 319 anomalies (RI residuals). The model uncertainties (the grey area) are characterized as the 25<sup>th</sup>-75<sup>th</sup> quantile range of RI residuals in non-  
 320 legacy years.

321 To complement the analysis of the legacy effects on GPP at the seasonal and annual scales, we also evaluated legacy effects  
 322 on tree growth at the annual scale. RI of *Fagus sylvatica* was below the 25<sup>th</sup> percentile of model residuals in the post-drought  
 323 year 2004 and returned to the 25<sup>th</sup>-75<sup>th</sup> percentiles of model residuals in 2005. For species of *Acer pseudoplatanus*, *Fraxinus*  
 324 *excelsior*, and others, residuals of RI were almost within 25<sup>th</sup>-75<sup>th</sup> percentiles of model residuals in 2004 and 2005. After the  
 325 2018 drought, RI of all species for 2019 and 2020 were almost within or close to 25<sup>th</sup>-75<sup>th</sup> percentiles of model residuals.  
 326

#### 327 4.6 Concurrent and lagged reduction in GPP



328  
 329 **Figure 7. Concurrent (dashed black bars) and lagged (colored bars) reduction in GPP from the 2003 and 2018 droughts at a) DE-**  
 330 **Hai and b) DE-Lnf.** Concurrent impacts in GPP were quantified as the sum of GPP anomalies over drought periods in drought years relative  
 331 to averaged total GPP over the growing season (see Method). Lagged impacts in GPP are characterized as the difference between GPP<sub>anom</sub>  
 332 residuals in legacy years and median of the model uncertainties relative to averaged total GPP over the growing season. Colored bars and  
 333 error bars show the median and 5-95%, respectively, of lagged reduction in GPP from ensemble model runs.

334 Finally, we compared the concurrent impacts on GPP with the lagged impacts due to drought. We found that, at DE-Hai, the  
 335 concurrent reduction in GPP was 9.4% relative to averaged total GPP over the growing season (hereinafter) in 2003, while  
 336 6.1-12.3% indirectly reduced in 2004. And in 2018 concurrent reduction in GPP was 21.0%, while 3.5%-10.0% and 23.5-  
 337 29.6% indirectly reduced in 2019 and 2020, respectively. At DE-Lnf, the concurrent reduction in GPP was negligible in 2003  
 338 (2.2%), while we estimated 14.4-24.8% GPP reduction in 2004, which was higher than the corresponding values at DE-Hai in  
 339 the same year.

340

## 341 **5. Discussion**

### 342 **5.1 A novel methodology to detect drought legacy effects on GPP**

343 There is limited research on discovering legacy effects of drought on the ecosystem carbon cycle using eddy-covariance  
344 observations (Kannenberget al., 2019). Here, we propose a residual-based methodology using a random-forest regression  
345 model to detect legacy effects on GPP, and found significant legacy effects on GPP using eddy-covariance data at two forests  
346 in central Germany in the similar climate but with different age and species composition. There are three advantages to our  
347 methodology: 1) capturing the temporal dynamics of legacy effects at the seasonal scales; 2) separating the influence of  
348 meteorological conditions during the post-drought period on recovery rates; 3) estimating model uncertainties to avoid  
349 misinterpreting small residuals as ‘legacy effects’.

350 First, because we used measurements with a high temporal resolution (daily), legacy effects could be determined across  
351 different time scales. Previous studies based on tree-ring or satellite-greenness data have mainly focused on legacy effects at  
352 the annual scale (Anderegg et al., 2015; Wu et al., 2018) or monthly scale (Bastos et al., 2021), but the legacies can be more  
353 ephemeral, for example, if they appear only in critical periods of the growing season, as we have found here. Such temporally  
354 confined effects may not necessarily manifest themselves at the annual scale. For example, after the 2003 drought, the annual  
355 GPP at DE-Hai in 2005 was close to normal, which was the 25<sup>th</sup> percentile of model residuals here, but we found short legacies  
356 at the seasonal scale (Fig. 3).

357 Second, recovery is usually considered when the target variable (i.e. GPP, tree-ring width...) returns to the baseline, usually  
358 based on pre-drought values of the target variable (Bose et al., 2020; González de Andrés et al., 2021; Zhang et al., 2021).  
359 However, meteorological conditions during the recovery period will modulate recovery rates, so that recovery can be delayed  
360 e.g. if a drought is followed by other unfavourable climatic conditions. Hence, the evaluation of possible legacy effects should  
361 be based on the functional relations between the target variable and meteorological conditions. Our model takes this into  
362 account by considering that ecosystems recovered when observed GPP reaches the potential GPP given the meteorological  
363 conditions, rather than the absolute flux.

364 Finally, our approach allows determining the uncertainties in estimated legacy effects. Previous studies (Anderegg et al., 2015;  
365 Huang et al., 2018) quantified legacy effects as the residuals between observed and predicted target variables (i.e. tree-ring  
366 width, vegetation indices, ...) in legacy years, but were not able to consider uncertainties of their trained models. Yet, it is  
367 crucial to understand if the residuals are caused by model uncertainties or can be interpreted as legacy effects. In this study,  
368 legacy effects are identified only when the model residuals are outside the range of the model uncertainties, so that we are  
369 confident that the legacies reported here are significant and avoid interpreting residuals caused by model error as legacy effects.  
370 A limitation of our approach is that we have to assume that there are no legacy effects in the climate system because this would  
371 potentially bias the interpretation of the residuals.



372 The methodology we proposed is able to detect the legacy effects of drought on GPP and can be easily applied to other eddy-  
373 covariance sites and variables (i.e. evapotranspiration, transpiration, ...), in order to improve our understanding of drought  
374 legacy effects on the ecosystem carbon cycle at different time-scales.

375

## 376 **5.2 Seasonal and annual legacy drought impacts on GPP**

377 We found that residuals of GPP anomalies ( $GPP_{anom}$  residuals) in legacy years were significantly larger than model  
378 uncertainties at both seasonal and annual scales at both sites, which indicated strong legacy effects of drought on GPP at least  
379 in the two years following the drought events.

380 We found negative legacies on GPP (reduced uptake) in the early growing season of all legacy years (2004, 2005, 2019, and  
381 2020) at DE-Hai. Reduced and delayed leaf development due to physiological effects of the 2003 and 2018 droughts (e.g.  
382 metabolic damage, non-structural carbohydrates depletion) could result in reduced ecosystem-level photosynthesis  
383 (Migliavacca et al., 2009; Rocha and Goulden, 2010; Kannenberg et al., 2019), and could potentially explain negative legacies  
384 on GPP at the start of the growing season. In line with this hypothesis, we found the enhanced vegetation index (EVI, a proxy  
385 of leaf area index, Fig. S5 and Fig. S6) at the sites showed lower values than other years in the early growing seasons of 2004,  
386 2005, and 2019 and this delayed spring phenology propagated over the year of 2004 and 2019 with a shift of seasonality. We  
387 found consistently lower values of NPP allocated to foliage growth in 2004 than other years (Fig. S7). Furthermore, the  
388 detected negative legacies in the early growing season became smaller when adding EVI anomalies as an additional predictor  
389 in the random forest model (Fig. 5), indicating that the reduced and delayed leaf development partly explained the estimated  
390 legacy effects by the RF model trained with climate predictors only.

391 Another possible mechanism explaining legacy effects could be hydraulic damage induced by drought (Anderegg et al., 2013),  
392 and therefore insufficient ability of water transport limiting sink strength (Körner, 2015) and photosynthetic capacity (Chen et  
393 al., 2010), at least until damage is repaired. If this was the case, transpiration fluxes should be reduced. However, we did not  
394 find similar negative legacy patterns on transpiration in the early growing season (Fig. S8a). Therefore, hydraulic damage did  
395 not seem a likely cause of drought legacies on GPP for these events. Overall, we cannot pinpoint the physiological causes of  
396 the detected legacy effects due to limited availability of measurements. This calls for establishing more plant-physiological  
397 measurements complementing eddy-covariance and RI measurements to capture sufficient information about plant water  
398 relations such as sap flow (Poyatos et al., 2021) and tree water deficit (Nehemy et al., 2021) as well as carbon allocation  
399 (Hartmann et al, 2020) to provide a more detailed process understanding of the mechanisms underlying drought legacy effects.  
400 Negative legacies on GPP in terms of lagged reduction in GPP in 2004 at DE-Lnf (14.4-24.8%) were stronger than those at  
401 DE-Hai (6.1-12.3%) in the seasonal and annual scales. The persistence of negative legacies throughout the full growing season  
402 in 2004 indicates that the 2003 drought likely caused stronger damage, especially reduced leaf development which was  
403 supported by largely reduced negative legacies of  $RF_{EVI}$  with EVI comparing to RF without EVI (Fig. 5), on the ecosystem at  
404 DE-Lnf than that at DE-Hai. From the community-level perspective, the stronger legacy effects found at DE-Lnf compared to

405 DE-Hai may have been partly related to differences in forest composition between the two sites (Tamrakar et al. 2018, Pardos  
406 et al., 2021). Measurements of GPP at tree species level were not available, therefore we relied on the legacies found for RI  
407 (reflecting growth), available for individual trees at DE-Hai. It should be noted, though, that the relationship between GPP and  
408 growth is complex (Fatichi et al., 2014). Negative legacy effects on RI of *Fagus sylvatica*, dominating at DE-Hai, in 2004,  
409 were found, whereas other co-dominating species (*Acer pseudoplatanus* and *Fraxinus excelsior*) did not show negative  
410 legacies. Therefore, the lower resilience of *Fagus sylvatica* compared to other species may have partly resulted in stronger  
411 negative legacies at the pure European beech forest at DE-Lnf than at DE-Hai. In addition, contrasting legacy effects of these  
412 two sites could also be associated with different age classes and the absolute stand age since the effects of stand age  
413 modulating the heat and drought impact on carbon exchange (Arain et al., 2022) and ecosystem-level photosynthetic capacity  
414 (Musavi et al., 2017) have been recognized. However, the evidence of species diversity and age structure effects on legacy  
415 effects needs to be further explored using more sites in the future.

416 Stronger negative legacy effects on GPP in 2020 than those in other legacy years were found at DE-Hai in the seasonal and  
417 annual scales. This might be associated with significant tree mortality in the whole forest including the main footprint in the  
418 period 2018-2020 (about 6% year<sup>-1</sup> between 2017 and 2020 compared to less than 1% year<sup>-1</sup> between 2005 and 2017) mainly  
419 caused by the storm *Friedrike* in January 2018 and the heat and/or drought in summer 2018 and 2019 (unpublished data). RI  
420 of *Fagus sylvatica* in 2020 showed slightly positive legacy effects in growth, since only living trees were sampled. This might  
421 be explained by the favorable weather conditions in winter/spring 2019/2020 associated with high mineralization rates and  
422 reduced competition for nutrients, light and water of the surviving trees (Grossiord, 2020). The RI data reflected mean growth  
423 signals from individual surviving trees, while the GPP data reflected mean carbon assimilation at stand level, including  
424 positive, negative or absent legacy effects at individual tree level as well as the reduction of assimilating individuals due to  
425 higher tree mortality.

426 Overall, we found that the lagged impacts of drought on GPP are significant compared with concurrent drought impacts at the  
427 two sites studied here. The lagged reduction in GPP resulting from drought is usually not quantified (Ciais et al., 2005;  
428 Reichstein et al., 2007), perhaps because separating legacy effects on ecosystem carbon fluxes from observations is challenging  
429 (Kannenberget al., 2019) and process-based models have been shown to miss such legacy effects (Bastos et al., 2021). This  
430 implies that the impact of droughts on ecosystem carbon cycling in most studies might be underestimated.

431

### 432 **5.3 Importance of deep root-zone soil moisture data**

433 Deep root-zone soil moisture has been recognized as an important water source for vegetation, especially during droughts  
434 (Miguez-Macho and Fan, 2021; Werner et al., 2021). Although soil moisture measurements across three soil layers are  
435 available at both sites, the deepest depth (ca. 30cm) cannot capture the entire soil water reservoir available for European beech  
436 which has been observed to have non-negligible amounts of fine roots below 30cm across different sites (Leuschner et al.,  
437 2004, Gessler et al., 2021).

438 We tested an initial model using anomalies of soil moisture at three layers as predictors (RF<sub>SM</sub>), and found strong positive  
439 legacy effects in the late growing season in 2019 at DE-Hai (Fig. S9), which however could not be reproduced by any of the  
440 models using soil moisture information from deeper layers (Fig. S9) including the local water balance (WAI, CWD) and the  
441 reanalysis data (ERA5). Comparing the predicted time series of GPP<sub>anom</sub> of the RF<sub>SM</sub> model with observations, we found the  
442 predicted GPP<sub>anom</sub> became much more negative in the late growing season while observed GPP<sub>anom</sub> were close to zero (Fig.  
443 S10). Therefore, although soil moisture anomalies in the third layer (30cm) were largely negative when the positive residuals  
444 appeared (Fig. S11), soil moisture from layers deeper than 30 cm may maintain the water supply for photosynthesis. Also, we  
445 found the evapotranspiration from the shallow layers (0~30cm) estimated by soil moisture decrease was less than the observed  
446 evapotranspiration during dry-down periods (Fig. S12), which indicated plant water uptake from layers deeper than 30 cm  
447 during dry-down periods, in line with our hypothesis. In summary, these positive patterns are likely due to model errors from  
448 incomplete information on the soil-moisture profile rather than actual positive legacy effects.  
449 These results highlight the importance of soil moisture measurements that capture the entire root zone for more reliable  
450 understanding of ecosystem functioning, particularly in the case of drought legacy effects.

## 451 **6. Conclusions**

452 The frequency, intensity, duration, and spatial extent of droughts are expected to increase in the next decades due to  
453 anthropogenically caused global warming in many regions (IPCC, 2022). Drought not only impacts ecosystems concurrently,  
454 but also can have legacy effects on ecosystem carbon fluxes. We developed a residual-based approach using a random forest  
455 regression model to detect drought legacies on gross primary productivity (GPP) using eddy-covariance data. The methodology  
456 proposed here allows quantifying significant drought legacy effects on GPP at the sub-seasonal and annual scales. The GPP  
457 reduction due to drought legacy effects is of comparable magnitude to the concurrent drought effects at the studied sites, which  
458 confirms the importance of legacy effects. We found contrasting legacy effects at two neighbouring forests with different  
459 species and age structures, yet the importance of these factors could not be evaluated. Future studies across a larger range of  
460 sites will be needed to understand whether the crucial role of legacy effects is general and on which mediating factors they  
461 depend.

## 463 **Acknowledgements**

464 Xin Yu and Markus Reichstein acknowledge funding from the European Research Council (ERC) Synergy Grant  
465 “Understanding and Modelling the Earth System with Machine Learning (USMILE)” under the Horizon 2020 research and  
466 innovation programme (Grant agreement No. 855187). Xin Yu acknowledges support from the International Max Planck  
467 Research School for Global Biogeochemical Cycles. René Orth acknowledges support by the German Research Foundation

468 (Emmy Noether grant 391059971). Franziska Koebsch and Alexander Knohl acknowledge support by Niedersächsisches  
469 Vorab (ZN 3679), Ministry of Lower-Saxony for Science and Culture (MWK). Martina Mund acknowledges support by the  
470 Integrated project CarboEurope-IP (European Commission, Directorate-General Research, Sixth Framework Programme,  
471 Priority 1.1.6.3: Global Change and Ecosystem, Contract no. GOCECT-2003-505572), the Max Planck Institute for  
472 Biogeochemistry, Germany, the German Research Foundation (DFG) (INST 186/1118-1 FUGG), the German Federal  
473 Ministry of Education and Research (BMBF; research infrastructure ICOS) and the Georg-August-University Göttingen,  
474 Germany. Sophia Walther acknowledges funding within the ESA Living Planet Fellowship on the project Vad3e mecum.  
475 Benjamin D. Stocker was funded by the Swiss National Science Foundation grant no. PCEFP2\_181115. We thank the Warm  
476 Winter 2020 initiative of the Integrated Carbon Observation System (ICOS), specifically Nicola Arriga and Dario Papale, and  
477 the administration of the Hainich National Park for the opportunity for research within the National Park.

#### 478 **Author contributions**

479 The study was conceived by X. Yu, A. Bastos, R. Orth, M. Reichstein, and M. Bahn. X. Yu implemented the method and  
480 performed the data analyses. A. Knohl, A. Klosterhalfen, and F. Koebsch provided the eddy-covariance data. M. Mund  
481 provided the data of radial increment and net primary productivity of fruits and leaves. J. A. Nelson helped X. Yu to process  
482 the transpiration estimation. S. Walther provided and processed the Enhanced Vegetation Index data. B. D. Stocker suggested  
483 quantitatively separating structural and physiological effects. M. Migliavacca helped to interpret the results. X. Yu, A. Bastos,  
484 R. Orth, M. Reichstein, and M. Bahn prepared the first draft and all authors contributed to discussion of results and the revisions  
485 of the manuscript.

486

#### 487 **Competing interests**

488 At least one of the (co-)authors is a member of the editorial board of Biogeosciences. The peer-review process should be  
489 guided by an independent editor, and the authors also have no other competing interests to declare.

#### 490 **Code and data availability**

491 Eddy-covariance and enhanced vegetation index data used are freely accessible. Tree ring width and net primary productivity  
492 of fruits and leaves data are available on request to Martina Mund. Our code is available on request.

493 **References**

- 494 Allen, C. D., Breshears, D. D., and McDowell, N. G.: On underestimation of global vulnerability to tree mortality and forest  
495 die-off from hotter drought in the Anthropocene, 6, art129, <https://doi.org/10.1890/ES15-00203.1>, 2015.
- 496 Anderegg, W. R. L., Plavcová, L., Anderegg, L. D. L., Hacke, U. G., Berry, J. A., and Field, C. B.: Drought's legacy: multiyear  
497 hydraulic deterioration underlies widespread aspen forest die-off and portends increased future risk, 19, 1188–1196,  
498 <https://doi.org/10.1111/gcb.12100>, 2013.
- 499 Anderegg, W. R. L., Schwalm, C., Biondi, F., Camarero, J. J., Koch, G., Litvak, M., Ogle, K., Shaw, J. D., Shevliakova, E.,  
500 Williams, A. P., Wolf, A., Ziaco, E., and Pacala, S.: Pervasive drought legacies in forest ecosystems and their implications for  
501 carbon cycle models, 349, 528–532, <https://doi.org/10.1126/science.aab1833>, 2015.
- 502 Anthoni, P. M., Knohl, A., Rebmann, C., Freibauer, A., Mund, M., Ziegler, W., Kolle, O., and Schulze, E.-D.: Forest and  
503 agricultural land-use-dependent CO<sub>2</sub> exchange in Thuringia, Germany, 10, 2005–2019, [https://doi.org/10.1111/j.1365-](https://doi.org/10.1111/j.1365-2486.2004.00863.x)  
504 [2486.2004.00863.x](https://doi.org/10.1111/j.1365-2486.2004.00863.x), 2004.
- 505 Arain, M. A., Xu, B., Brodeur, J. J., Khomik, M., Peichl, M., Beamesderfer, E., Restrepo-Couple, N., and Thorne, R.: Heat  
506 and drought impact on carbon exchange in an age-sequence of temperate pine forests, *Ecological Processes*, 11, 7,  
507 <https://doi.org/10.1186/s13717-021-00349-7>, 2022.
- 508 Assal, T. J., Anderson, P. J., and Sibold, J.: Spatial and temporal trends of drought effects in a heterogeneous semi-arid forest  
509 ecosystem, *Forest Ecology and Management*, 365, 137–151, <https://doi.org/10.1016/j.foreco.2016.01.017>, 2016.
- 510 Aubinet, M., Grelle, A., Ibrom, A., Rannik, U., Moncrieff, J., Foken, T., Kowalski, A. S., Martin, P. H., Berbigier, P.,  
511 Grunwald, T., Morgenstern, K., Pilegaard, K., Rebmann, C., Bernhofer, C., Clement, R., Elbers, J., Granier, A., Snijders, W.,  
512 Valentini, R., and Vesala, T.: Estimates of the Annual Net Carbon and Water Exchange, 30, 113–174, 2000.
- 513 Bastos, A., Orth, R., Reichstein, M., Ciais, P., Viovy, N., Zaehle, S., Anthoni, P., Arneth, A., Gentine, P., Joetzjer, E., Lienert,  
514 S., Loughran, T., McGuire, P. C., O, S., Pongratz, J., and Sitch, S.: Vulnerability of European ecosystems to two compound  
515 dry and hot summers in 2018 and 2019, 12, 1015–1035, <https://doi.org/10.5194/esd-12-1015-2021>, 2021.
- 516 Beringer, J., Hutley, L. B., Tapper, N. J., and Cernusak, L. A.: Savanna fires and their impact on net ecosystem productivity  
517 in North Australia, *Global Change Biol*, 13, 990–1004, <https://doi.org/10.1111/j.1365-2486.2007.01334.x>, 2007.
- 518 Bose, A. K., Gessler, A., Bolte, A., Bottero, A., Buras, A., Cailleret, M., Camarero, J. J., Haeni, M., Hereş, A.-M., Hevia, A.,  
519 Lévesque, M., Linares, J. C., Martinez-Vilalta, J., Matías, L., Menzel, A., Sánchez-Salguero, R., Saurer, M., Vennetier, M.,  
520 Ziche, D., and Rigling, A.: Growth and resilience responses of Scots pine to extreme droughts across Europe depend on  
521 predrought growth conditions, 26, 4521–4537, <https://doi.org/10.1111/gcb.15153>, 2020.
- 522 Breiman, L.: Random Forests, *Machine Learning*, 45, 5–32, <https://doi.org/10.1023/A:1010933404324>, 2001.
- 523 Chen, J.-W., Zhang, Q., Li, X.-S., and Cao, K.-F.: Gas exchange and hydraulics in seedlings of *Hevea brasiliensis* during water  
524 stress and recovery, *Tree Physiology*, 30, 876–885, <https://doi.org/10.1093/treephys/tpq043>, 2010.

525 Ciais, P., Reichstein, M., Viovy, N., Granier, A., Ogee, J., Allard, V., Aubinet, M., Buchmann, N., Bernhofer, C., Carrara, A.,  
526 Chevallier, F., De Noblet, N., Friend, A. D., Friedlingstein, P., Grünwald, T., Heinesch, B., Keronen, P., Knohl, A., Krinner,  
527 G., Loustau, D., Manca, G., Matteucci, G., Miglietta, F., Ourcival, J. M., Papale, D., Pilegaard, K., Rambal, S., Seufert, G.,  
528 Soussana, J. F., Sanz, M. J., Schulze, E. D., Vesala, T., and Valentini, R.: Europe-wide reduction in primary productivity  
529 caused by the heat and drought in 2003, 437, 529–533, <https://doi.org/10.1038/nature03972>, 2005.

530 Erbilgin, N., Zanganeh, L., Klutsch, J. G., Chen, S., Zhao, S., Ishangulyyeva, G., Burr, S. J., Gaylord, M., Hofstetter, R.,  
531 Keefover-Ring, K., Raffa, K. F., and Kolb, T.: Combined drought and bark beetle attacks deplete non-structural carbohydrates  
532 and promote death of mature pine trees, 44, 3866–3881, <https://doi.org/10.1111/pce.14197>, 2021.

533 Fatichi, S., Leuzinger, S., and Körner, C.: Moving beyond photosynthesis: from carbon source to sink-driven vegetation  
534 modeling, 201, 1086–1095, <https://doi.org/10.1111/nph.12614>, 2014.

535 Frank, D., Reichstein, M., Bahn, M., Thonicke, K., Frank, D., Mahecha, M. D., Smith, P., Velde, M. van der, Vicca, S., Babst,  
536 F., Beer, C., Buchmann, N., Canadell, J. G., Ciais, P., Cramer, W., Ibrom, A., Miglietta, F., Poulter, B., Rammig, A.,  
537 Seneviratne, S. I., Walz, A., Wattenbach, M., Zavala, M. A., and Zscheischler, J.: Effects of climate extremes on the terrestrial  
538 carbon cycle: concepts, processes and potential future impacts, 21, 2861–2880, <https://doi.org/10.1111/gcb.12916>, 2015.

539 Fu, Z., Ciais, P., Bastos, A., Stoy, P. C., Yang, H., Green, J. K., Wang, B., Yu, K., Huang, Y., Knohl, A., Šigut, L., Gharun,  
540 M., Cuntz, M., Arriga, N., Roland, M., Peichl, M., Migliavacca, M., Cremonese, E., Varlagin, A., Brümmer, C., Gourlez de la  
541 Motte, L., Fares, S., Buchmann, N., El-Madany, T. S., Pitacco, A., Vendrame, N., Li, Z., Vincke, C., Magliulo, E., and  
542 Koepsch, F.: Sensitivity of gross primary productivity to climatic drivers during the summer drought of 2018 in Europe, 375,  
543 20190747, <https://doi.org/10.1098/rstb.2019.0747>, 2020.

544 Galvagno, M., Wohlfahrt, G., Cremonese, E., Rossini, M., Colombo, R., Filippa, G., Julitta, T., Manca, G., Siniscalco, C.,  
545 Cella, U. M. di, and Migliavacca, M.: Phenology and carbon dioxide source/sink strength of a subalpine grassland in response  
546 to an exceptionally short snow season, *Environ. Res. Lett.*, 8, 025008, <https://doi.org/10.1088/1748-9326/8/2/025008>, 2013.

547 Gessler, A., Bächli, L., Rouholahnejad Freund, E., Treydte, K., Schaub, M., Haeni, M., Weiler, M., Seeger, S., Marshall, J.,  
548 and Hug, C.: Drought reduces water uptake in beech from the drying topsoil, but no compensatory uptake occurs from deeper  
549 soil layers, *New Phytologist*, 2021.

550 González de Andrés, E., Rosas, T., Camarero, J. J., and Martínez-Vilalta, J.: The intraspecific variation of functional traits  
551 modulates drought resilience of European beech and pubescent oak, 109, 3652–3669, <https://doi.org/10.1111/1365-2745.13743>, 2021.

552

553 Grossiord, C.: Having the right neighbors: how tree species diversity modulates drought impacts on forests, 228, 42–49,  
554 <https://doi.org/10.1111/nph.15667>, 2020.

555 Haberstroh, S. and Werner, C.: The role of species interactions for forest resilience to drought, n/a,  
556 <https://doi.org/10.1111/plb.13415>, 2022.

557 Hackett-Pain, A. J., Friend, A. D., Lagueard, J. G. A., and Thomas, P. A.: The influence of masting phenomenon on growth–  
558 climate relationships in trees: explaining the influence of previous summers’ climate on ring width, *Tree Physiology*, 35, 319–  
559 330, <https://doi.org/10.1093/treephys/tpv007>, 2015.

560 Hartmann, H. and Trumbore, S.: Understanding the roles of nonstructural carbohydrates in forest trees – from what we can  
561 measure to what we want to know, 211, 386–403, <https://doi.org/10.1111/nph.13955>, 2016.

562 Hartmann, H., Bahn, M., Carbone, M., and Richardson, A. D.: Plant carbon allocation in a changing world – challenges and  
563 progress: introduction to a Virtual Issue on carbon allocation, 227, 981–988, <https://doi.org/10.1111/nph.16757>, 2020.

564 Herbst, M., Mund, M., Tamrakar, R., and Knohl, A.: Differences in carbon uptake and water use between a managed and an  
565 unmanaged beech forest in central Germany, *Forest Ecology and Management*, 355, 101–108,  
566 <https://doi.org/10.1016/j.foreco.2015.05.034>, 2015.

567 Huang, J., Hammerbacher, A., Gershenzon, J., Dam, N. M. van, Sala, A., McDowell, N. G., Chowdhury, S., Gleixner, G.,  
568 Trumbore, S., and Hartmann, H.: Storage of carbon reserves in spruce trees is prioritized over growth in the face of carbon  
569 limitation, *PNAS*, 118, <https://doi.org/10.1073/pnas.2023297118>, 2021.

570 Huang, M., Wang, X., Keenan, T. F., and Piao, S.: Drought timing influences the legacy of tree growth recovery, 24, 3546–  
571 3559, <https://doi.org/10.1111/gcb.14294>, 2018.

572 IPCC, 2022: Climate Change 2022: Impacts, Adaptation, and Vulnerability. Contribution of Working Group II to the Sixth  
573 Assessment Report of the Intergovernmental Panel on Climate Change [H.-O. Pörtner, D.C. Roberts, M. Tignor, E.S.  
574 Poloczanska, K. Mintenbeck, A. Alegría, M. Craig, S. Langsdorf, S. Lösschke, V. Möller, A. Okem, B. Rama (eds.)].  
575 Cambridge University Press. In Press.

576 Kannenberg, S. A., Novick, K. A., Alexander, M. R., Maxwell, J. T., Moore, D. J. P., Phillips, R. P., and Anderegg, W. R. L.:  
577 Linking drought legacy effects across scales: From leaves to tree rings to ecosystems, 25, 2978–2992,  
578 <https://doi.org/10.1111/gcb.14710>, 2019.

579 Kannenberg, S. A., Schwalm, C. R., and Anderegg, W. R. L.: Ghosts of the past: how drought legacy effects shape forest  
580 functioning and carbon cycling, 23, 891–901, <https://doi.org/10.1111/ele.13485>, 2020.

581 Kendall, M. G.: Rank correlation methods., 1948.

582 Knohl, A., Schulze, E.-D., Kolle, O., and Buchmann, N.: Large carbon uptake by an unmanaged 250-year-old deciduous forest  
583 in Central Germany, *Agricultural and Forest Meteorology*, 118, 151–167, [https://doi.org/10.1016/S0168-1923\(03\)00115-1](https://doi.org/10.1016/S0168-1923(03)00115-1),  
584 2003.

585 Körner, C.: Paradigm shift in plant growth control, *Current Opinion in Plant Biology*, 25, 107–114,  
586 <https://doi.org/10.1016/j.pbi.2015.05.003>, 2015.

587 Krishnan, P., Black, T. A., Grant, N. J., Barr, A. G., Hogg, E. (Ted) H., Jassal, R. S., and Morgenstern, K.: Impact of changing  
588 soil moisture distribution on net ecosystem productivity of a boreal aspen forest during and following drought, *Agricultural  
589 and Forest Meteorology*, 139, 208–223, <https://doi.org/10.1016/j.agrformet.2006.07.002>, 2006.

590 Leuschner, C., Hertel, D., Schmid, I., Koch, O., Muhs, A., and Hölscher, D.: Stand fine root biomass and fine root morphology  
591 in old-growth beech forests as a function of precipitation and soil fertility, *Plant and Soil*, 258, 43–56,  
592 <https://doi.org/10.1023/B:PLSO.0000016508.20173.80>, 2004.

593 Lewis, S. L., Brando, P. M., Phillips, O. L., van der Heijden, G. M. F., and Nepstad, D.: The 2010 Amazon Drought, 331, 554–  
594 554, <https://doi.org/10.1126/science.1200807>, 2011.

595 Ma, X., Huete, A., Moran, S., Ponce-Campos, G., and Eamus, D.: Abrupt shifts in phenology and vegetation productivity  
596 under climate extremes, 120, 2036–2052, <https://doi.org/10.1002/2015JG003144>, 2015.

597 Meinshausen, N., & Ridgeway, G. (2006). Quantile regression forests. *Journal of Machine Learning Research*, 7(6).

598 Migliavacca, M., Meroni, M., Manca, G., Matteucci, G., Montagnani, L., Grassi, G., Zenone, T., Teobaldelli, M., Goded, I.,  
599 Colombo, R., and Seufert, G.: Seasonal and interannual patterns of carbon and water fluxes of a poplar plantation under  
600 peculiar eco-climatic conditions, *Agricultural and Forest Meteorology*, 149, 1460–1476,  
601 <https://doi.org/10.1016/j.agrformet.2009.04.003>, 2009.

602 Miguez-Macho, G. and Fan, Y.: Spatiotemporal origin of soil water taken up by vegetation, 598, 624–628,  
603 <https://doi.org/10.1038/s41586-021-03958-6>, 2021.

604 Müller, L. M. and Bahn, M.: Drought legacies and ecosystem responses to subsequent drought, *Global Change Biology*, 28,  
605 5086–5103, <https://doi.org/10.1111/gcb.16270>, 2022.

606 Mund, M., Herbst, M., Knohl, A., Matthäus, B., Schumacher, J., Schall, P., Siebicke, L., Tamrakar, R., and Ammer, C.: It is  
607 not just a ‘trade-off’: indications for sink- and source-limitation to vegetative and regenerative growth in an old-growth beech  
608 forest, 226, 111–125, <https://doi.org/10.1111/nph.16408>, 2020.

609 Musavi, T., Migliavacca, M., Reichstein, M., Kattge, J., Wirth, C., Black, T. A., Janssens, I., Knohl, A., Loustau, D., Rouspard,  
610 O., Varlagin, A., Rambal, S., Cescatti, A., Gianelle, D., Kondo, H., Tamrakar, R., and Mahecha, M. D.: Stand age and species  
611 richness dampen interannual variation of ecosystem-level photosynthetic capacity, *Nat Ecol Evol*, 1, 1–7,  
612 <https://doi.org/10.1038/s41559-016-0048>, 2017.

613 Nehemy, M. F., Benettin, P., Asadollahi, M., Pratt, D., Rinaldo, A., and McDonnell, J. J.: Tree water deficit and dynamic  
614 source water partitioning, 35, e14004, <https://doi.org/10.1002/hyp.14004>, 2021.

615 Nelson, J. A., Carvalhais, N., Cuntz, M., Delpierre, N., Knauer, J., Ogée, J., Migliavacca, M., Reichstein, M., and Jung, M.:  
616 Coupling Water and Carbon Fluxes to Constrain Estimates of Transpiration: The TEA Algorithm, 123, 3617–3632,  
617 <https://doi.org/10.1029/2018JG004727>, 2018.

618 Orth, R., Destouni, G., Jung, M., and Reichstein, M.: Large-scale biospheric drought response intensifies linearly with drought  
619 duration in arid regions, 17, 2647–2656, <https://doi.org/10.5194/bg-17-2647-2020>, 2020.

620 Pardos, M., del Río, M., Pretzsch, H., Jactel, H., Bielak, K., Bravo, F., Brazaitis, G., Defossez, E., Engel, M., Godvod, K.,  
621 Jacobs, K., Jansone, L., Jansons, A., Morin, X., Nothdurft, A., Oreti, L., Ponette, Q., Pach, M., Riofrío, J., Ruíz-Peinado, R.,



622 Tomao, A., Uhl, E., and Calama, R.: The greater resilience of mixed forests to drought mainly depends on their composition:  
623 Analysis along a climate gradient across Europe, *Forest Ecology and Management*, 481, 118687,  
624 <https://doi.org/10.1016/j.foreco.2020.118687>, 2021.

625 Pastorello, G., Trotta, C., Canfora, E., Chu, H., Christianson, D., Cheah, Y.-W., Poindexter, C., Chen, J., Elbashandy, A.,  
626 Humphrey, M., Isaac, P., Polidori, D., Reichstein, M., Ribeca, A., van Ingen, C., Vuichard, N., Zhang, L., Amiro, B., Ammann,  
627 C., Arain, M. A., Ardö, J., Arkebauer, T., Arndt, S. K., Arriga, N., Aubinet, M., Aurela, M., Baldocchi, D., Barr, A.,  
628 Beamesderfer, E., Marchesini, L. B., Bergeron, O., Beringer, J., Bernhofer, C., Berveiller, D., Billesbach, D., Black, T. A.,  
629 Blanken, P. D., Bohrer, G., Boike, J., Bolstad, P. V., Bonal, D., Bonnefond, J.-M., Bowling, D. R., Bracho, R., Brodeur, J.,  
630 Brümmer, C., Buchmann, N., Burban, B., Burns, S. P., Buysse, P., Cale, P., Cavagna, M., Cellier, P., Chen, S., Chini, I.,  
631 Christensen, T. R., Cleverly, J., Collalti, A., Consalvo, C., Cook, B. D., Cook, D., Coursolle, C., Cremonese, E., Curtis, P. S.,  
632 D'Andrea, E., da Rocha, H., Dai, X., Davis, K. J., Cinti, B. D., Grandcourt, A. de Ligne, A. D., De Oliveira, R. C., Delpierre,  
633 N., Desai, A. R., Di Bella, C. M., Tommasi, P. di, Dolman, H., Domingo, F., Dong, G., Dore, S., Duce, P., Dufrêne, E., Dunn,  
634 A., Dušek, J., Eamus, D., Eichelmann, U., ElKhidir, H. A. M., Eugster, W., Ewenz, C. M., Ewers, B., Famulari, D., Fares, S.,  
635 Feigenwinter, I., Feitz, A., Fensholt, R., Filippa, G., Fischer, M., Frank, J., Galvagno, M., et al.: The FLUXNET2015 dataset  
636 and the ONEFlux processing pipeline for eddy covariance data, *Sci Data*, 7, 225, <https://doi.org/10.1038/s41597-020-0534-3>,  
637 2020.

638 Peltier, D. M. P., Guo, J., Nguyen, P., Bangs, M., Wilson, M., Samuels-Crow, K., Yocom, L. L., Liu, Y., Fell, M. K., Shaw,  
639 J. D., Auty, D., Schwalm, C., Anderegg, W. R. L., Koch, G. W., Litvak, M. E., and Ogle, K.: Temperature memory and non-  
640 structural carbohydrates mediate legacies of a hot drought in trees across the southwestern US, *Tree Physiology*,  
641 <https://doi.org/10.1093/treephys/tpab091>, 2021.

642 Piao, S., Zhang, X., Chen, A., Liu, Q., Lian, X., Wang, X., Peng, S., and Wu, X.: The impacts of climate extremes on the  
643 terrestrial carbon cycle: A review, *Sci. China Earth Sci.*, 62, 1551–1563, <https://doi.org/10.1007/s11430-018-9363-5>, 2019.

644 Poyatos, R., Granda, V., Flo, V., Adams, M. A., Adorján, B., Aguadé, D., Aidar, M. P. M., Allen, S., Alvarado-Barrientos, M.  
645 S., Anderson-Teixeira, K. J., Aparecido, L. M., Arain, M. A., Aranda, I., Asbjornsen, H., Baxter, R., Beamesderfer, E., Berry,  
646 Z. C., Berveiller, D., Blakely, B., Boggs, J., Bohrer, G., Bolstad, P. V., Bonal, D., Bracho, R., Brito, P., Brodeur, J., Casanoves,  
647 F., Chave, J., Chen, H., Cisneros, C., Clark, K., Cremonese, E., Dang, H., David, J. S., David, T. S., Delpierre, N., Desai, A.  
648 R., Do, F. C., Dohnal, M., Domec, J.-C., Dzikiti, S., Edgar, C., Eichstaedt, R., El-Madany, T. S., Elbers, J., Eller, C. B.,  
649 Euskirchen, E. S., Ewers, B., Fonti, P., Forner, A., Forrester, D. I., Freitas, H. C., Galvagno, M., Garcia-Tejera, O., Ghimire,  
650 C. P., Gimeno, T. E., Grace, J., Granier, A., Griebel, A., Guanyu, Y., Gush, M. B., Hanson, P. J., Hasselquist, N. J., Heinrich,  
651 I., Hernandez-Santana, V., Herrmann, V., Hölttä, T., Holwerda, F., Irvine, J., Isarangkool Na Ayutthaya, S., Jarvis, P. G.,  
652 Jochheim, H., Joly, C. A., Kaplick, J., Kim, H. S., Klemetsson, L., Kropp, H., Lagergren, F., Lane, P., Lang, P., Lapenas, A.,  
653 Lechuga, V., Lee, M., Leuschner, C., Limousin, J.-M., Linares, J. C., Linderson, M.-L., Lindroth, A., Llorens, P., López-  
654 Bernal, Á., Loranty, M. M., Lüttschwager, D., Macinnis-Ng, C., Maréchaux, I., Martin, T. A., Matheny, A., McDowell, N.,

655 McMahon, S., Meir, P., et al.: Global transpiration data from sap flow measurements: the SAPFLUXNET database, 13, 2607–  
656 2649, <https://doi.org/10.5194/essd-13-2607-2021>, 2021.

657 Reichstein, M., Falge, E., Baldocchi, D., Papale, D., Aubinet, M., Berbigier, P., Bernhofer, C., Buchmann, N., Gilmanov, T.,  
658 Granier, A., Grünwald, T., Havránková, K., Ilvesniemi, H., Janous, D., Knohl, A., Laurila, T., Lohila, A., Loustau, D.,  
659 Matteucci, G., Meyers, T., Miglietta, F., Ourcival, J.-M., Pumpanen, J., Rambal, S., Rotenberg, E., Sanz, M., Tenhunen, J.,  
660 Seufert, G., Vaccari, F., Vesala, T., Yakir, D., and Valentini, R.: On the separation of net ecosystem exchange into assimilation  
661 and ecosystem respiration: review and improved algorithm, 11, 1424–1439, <https://doi.org/10.1111/j.1365-2486.2005.001002.x>, 2005.

663 Reichstein, M., Ciais, P., Papale, D., Valentini, R., Running, S., Viovy, N., Cramer, W., Granier, A., Ogee, J., Allard, V.,  
664 Aubinet, M., Bernhofer, C., Buchmann, N., Carrara, A., Grünwald, T., Heimann, M., Heinesch, B., Knohl, A., Kutsch, W.,  
665 Loustau, D., Manca, G., Matteucci, G., Miglietta, F., Ourcival, J. M., Pilegaard, K., Pumpanen, J., Rambal, S., Schaphoff, S.,  
666 Seufert, G., Soussana, J.-F., Sanz, M.-J., Vesala, T., and Zhao, M.: Reduction of ecosystem productivity and respiration during  
667 the European summer 2003 climate anomaly: a joint flux tower, remote sensing and modelling analysis, 13, 634–651,  
668 <https://doi.org/10.1111/j.1365-2486.2006.01224.x>, 2007.

669 Reichstein, M., Bahn, M., Ciais, P., Frank, D., Mahecha, M. D., Seneviratne, S. I., Zscheischler, J., Beer, C., Buchmann, N.,  
670 Frank, D. C., Papale, D., Rammig, A., Smith, P., Thonicke, K., van der Velde, M., Vicca, S., Walz, A., and Wattenbach, M.:  
671 Climate extremes and the carbon cycle, 500, 287–295, <https://doi.org/10.1038/nature12350>, 2013.

672 Rocha, A. V. and Goulden, M. L.: Drought legacies influence the long-term carbon balance of a freshwater marsh, 115,  
673 <https://doi.org/10.1029/2009JG001215>, 2010.

674 Ryo, M. and Rillig, M. C.: Statistically reinforced machine learning for nonlinear patterns and variable interactions, 8, e01976,  
675 <https://doi.org/10.1002/ecs2.1976>, 2017.

676 Schwalm, C. R., Williams, C. A., Schaefer, K., Arneeth, A., Bonal, D., Buchmann, N., Chen, J., Law, B. E., Lindroth, A.,  
677 Luyssaert, S., Reichstein, M., and Richardson, A. D.: Assimilation exceeds respiration sensitivity to drought: A FLUXNET  
678 synthesis, 16, 657–670, <https://doi.org/10.1111/j.1365-2486.2009.01991.x>, 2010.

679 Sun, S., Sun, G., Caldwell, P., McNulty, S., Cohen, E., Xiao, J., and Zhang, Y.: Drought impacts on ecosystem functions of  
680 the U.S. National Forests and Grasslands: Part II assessment results and management implications, *Forest Ecology and*  
681 *Management*, 353, 269–279, <https://doi.org/10.1016/j.foreco.2015.04.002>, 2015.

682 Tamrakar, R., Rayment, M. B., Moyano, F., Mund, M., and Knohl, A.: Implications of structural diversity for seasonal and  
683 annual carbon dioxide fluxes in two temperate deciduous forests, *Agricultural and Forest Meteorology*, 263, 465–476,  
684 <https://doi.org/10.1016/j.agrformet.2018.08.027>, 2018.

685 Tramontana, G., Jung, M., Schwalm, C. R., Ichii, K., Camps-Valls, G., Ráduly, B., Reichstein, M., Arain, M. A., Cescatti, A.,  
686 Kiely, G., Merbold, L., Serrano-Ortiz, P., Sickert, S., Wolf, S., and Papale, D.: Predicting carbon dioxide and energy fluxes  
687 across global FLUXNET sites with regression algorithms, 13, 4291–4313, <https://doi.org/10.5194/bg-13-4291-2016>, 2016.

688 Walther, S., Besnard, S., Nelson, J. A., El-Madany, T. S., Migliavacca, M., Weber, U., Ermida, S. L., Brümmer, C., Schrader,  
689 F., Prokushkin, A. S., Panov, A. V., and Jung, M.: Technical note: A view from space on global flux towers by MODIS and  
690 Landsat: The FluxnetEO dataset, *Biogeochemistry: Land*, <https://doi.org/10.5194/bg-2021-314>, 2021.

691 Wang, B., Chen, T., Li, C., Xu, G., Wu, G., and Liu, G.: Discrepancy in growth resilience to drought among different stand-  
692 aged forests declines going from a semi-humid region to an arid region, *Forest Ecology and Management*, 511, 120135,  
693 <https://doi.org/10.1016/j.foreco.2022.120135>, 2022.

694 Warm Winter 2020 Team, & ICOS Ecosystem Thematic Centre. (2022). Warm Winter 2020 ecosystem eddy covariance flux  
695 product for 73 stations in FLUXNET-Archive format—release 2022-1 (Version 1.0). ICOS Carbon Portal.  
696 <https://doi.org/10.18160/2G60-ZHAK>.

697 Werner, C., Meredith, L. K., Ladd, S. N., Ingrisch, J., Kübert, A., van Haren, J., Bahn, M., Bailey, K., Bamberger, I., Beyer,  
698 M., Blomdahl, D., Byron, J., Daber, E., Deleeuw, J., Dippold, M. A., Fudyma, J., Gil-Loaiza, J., Honeker, L. K., Hu, J., Huang,  
699 J., Klüpfel, T., Krechmer, J., Kreuzwieser, J., Kühnhammer, K., Lehmann, M. M., Meeran, K., Misztal, P. K., Ng, W.-R.,  
700 Pfannerstill, E., Pugliese, G., Purser, G., Roscioli, J., Shi, L., Tfaily, M., and Williams, J.: Ecosystem fluxes during drought  
701 and recovery in an experimental forest, 374, 1514–1518, <https://doi.org/10.1126/science.abj6789>, 2021.

702 Wu, X., Liu, H., Li, X., Ciais, P., Babst, F., Guo, W., Zhang, C., Magliulo, V., Pavelka, M., Liu, S., Huang, Y., Wang, P., Shi,  
703 C., and Ma, Y.: Differentiating drought legacy effects on vegetation growth over the temperate Northern Hemisphere, 24, 504–  
704 516, <https://doi.org/10.1111/gcb.13920>, 2018.

705 Zhang, S., Yang, Y., Wu, X., Li, X., and Shi, F.: Postdrought Recovery Time Across Global Terrestrial Ecosystems, *Journal*  
706 *of Geophysical Research: Biogeosciences*, 126, e2020JG005699, 2021.

707 Zscheischler, J., Mahecha, M. D., Buttler, J. von, Harmeling, S., Jung, M., Rammig, A., Randerson, J. T., Schölkopf, B.,  
708 Seneviratne, S. I., Tomelleri, E., Zaehle, S., and Reichstein, M.: A few extreme events dominate global interannual variability  
709 in gross primary production, *Environ. Res. Lett.*, 9, 035001, <https://doi.org/10.1088/1748-9326/9/3/035001>, 2014.